Interplanetary and solar surface properties of coronal holes observed during solar maximum

J. Zhang,[1,2] J. Woch,[1] S. K. Solanki,[1] R. von Steiger,[3] and R. Forsyth[4]

Received 17 June 2002; revised 29 November 2002; accepted 22 January 2003; published 4 April 2003.

[1] Data from the Solar Wind Ion Composition Spectrometer (SWICS) on board the Ulysses spacecraft and synoptic maps from Kitt Peak are used to analyze the relatively short-lived coronal holes which exist during the maximum phase of the solar activity cycle 23. They are compared with the persistent polar coronal holes which prevail around solar minimum. A solar wind velocity increase coinciding with a shift of the ionic charge composition toward lower charge states serves as a robust criterion for identifying solar wind streams emanating from solar maximum holes. This allows an unambiguous association of every stream identified in interplanetary space with a coronal hole on the solar surface with consistent magnetic polarity. Solar wind streams emanating from the solar maximum holes generally show lower velocities of 400 to 600 km/s compared to the polar hole stream velocities of 700 to 800 km/s. However, the SWICS O^{7+}/O^{6+} charge-state ratios, which are a proxy for coronal temperatures, do not reveal a consistent difference. Though a number of solar maximum holes have a significantly, up to three times, higher temperature compared to the polar coronal holes, the majority of the investigated holes and specifically those with new cycle polarity have a coronal temperature within the range of polar hole temperatures. Likewise, the magnetic flux density in the solar maximum holes and in the polar coronal holes, as derived from the synoptic maps, is not strikingly different. Therefore any intrinsic difference between solar maximum holes and polar coronal holes is small. The striking discrepancy in their kinetic properties, namely the slower velocity of the solar wind streams emanating from solar maximum holes, may partly be attributed to deceleration of the solar wind during propagation to the spacecraft. The discrepancy may also be influenced by active regions in close proximity to the coronal holes, which presumably is more likely for smaller holes. There may, however, be a tendency for the faster wind streams to emanate from cooler holes. *INDEX TERMS:* 7511 Solar Physics, Astrophysics, and Astronomy: Coronal holes; 2164 Interplanetary Physics: Solar wind plasma; 2169 Interplanetary Physics: Sources of the solar wind; 7536 Solar Physics, Astrophysics, and Astronomy: Solar activity cycle (2162); *KEYWORDS:* solar coronal holes, solar wind, coronal temperature, solar cycle variations

Citation: Zhang, J., J. Woch, S. K. Solanki, R. von Steiger, and R. Forsyth, Interplanetary and solar surface properties of coronal holes observed during solar maximum, *J. Geophys. Res.*, *108*(A4), 1144, doi:10.1029/2002JA009538, 2003.

1. Introduction

[2] Coronal holes are magnetically open regions of the Sun. Their intrinsic properties and their evolution with time are not only important for understanding the nature of the solar magnetic field, solar wind acceleration and heating, but also because of their influence on the geomagnetic environment, since they constitute the dominant source of the interplanetary magnetic field (IMF) and the near-ecliptic solar wind [*Wang et al.*, 1997; *Luhman et al.*, 2002]. The simplest geometric configuration prevails around solar minimum, with unipolar magnetic field regions and stable large polar coronal holes at both poles. As the Sun approaches activity maximum these polar coronal holes diminish in size and finally vanish. Instead, small scale holes appear at all latitudes, including relatively short-lived, small-scale holes at polar latitudes.

[3] The basic properties of coronal holes have been known for decades. The temperature of the corona is reduced in the coronal holes compared to the surrounding regions, and coronal holes are the source of the high-speed solar wind [*Krieger et al.*, 1973]. The interplanetary observations of coronal hole streams by the Ulysses spacecraft and the capabilities for diagnosing the corona provided by the telescopes on the Solar and Heliospheric Observatory

[1]Max-Planck-Institut für Aeronomie, Katlenburg-Lindau, Germany.
[2]Also at National Astronomical Observatories, Chinese Academy of Sciences, Beijing, China.
[3]International Space Science Institute, Bern, Switzerland.
[4]Blackett Laboratory, Imperial College, England, UK.

0148-0227/03/2002JA009538$09.00

(SOHO) offer improved possibilities to study coronal hole properties and their evolution over the solar cycle.

[4] Ulysses, on its polar orbit around the Sun, not only allows properties of coronal hole streams to be investigated in interplanetary space, but also coronal properties in the source region of the solar wind streams to be derived. The ionic composition is a reliable diagnostic for conditions in the solar wind source region. The first out-of-ecliptic observations of the solar minimum polar coronal holes confirmed the unipolar character of the coronal hole magnetic field and that the polar coronal holes are the source of an extremely stable and uniform high speed solar wind with velocities of about 750 km/s [*Forsyth et al.*, 1996; *Woch et al.*, 1997; *McComas et al.*, 2000]. The freezing-in temperature, a proxy for coronal temperature, derived from ionic charge-state ratios, is considerably lower in the fast wind originating from polar coronal holes than in the slow wind originating from the streamer belt. The O^{7+}/O^{6+} ratios indicate a temperature of about 1 MK in the polar coronal holes compared to temperatures exceeding 1.5 MK in the corona underlying the transient wind [*von Steiger et al.*, 2000]. A small but significant hemispherical asymmetry exists, with the north polar hole being cooler than the southern one [*Zhang et al.*, 2002]. However, there is no evidence of a significant evolution of coronal hole temperature over the solar cycle. Likewise, ground-based synoptic maps reflect a north-south asymmetry during the minimum between cycles 22 and 23, in that the northern polar coronal hole covers a larger part of the solar surface than the southern one. The total magnetic flux and, specifically, the flux density of the north polar coronal hole is considerably lower for the whole interval of time between 1992 and 1997.

[5] Recently, *McComas et al.* [2002] used Ulysses solar wind plasma and ion composition data to study a limited number of solar wind streams assumed to emanate from small-scale coronal holes which existed at high latitudes near solar maximum. They found that the ionic composition of these streams is comparable to that of the wind emanating from the solar minimum polar holes. However, the solar wind speed of the streams may differ considerably from that of the polar hole wind. They concluded that coronal holes, regardless of whether they are small-scale solar maximum ones or large-scale polar minimum holes, produce a unique type of solar wind. Consequently, these holes have similar chromospheric and coronal properties and, specifically, similar coronal temperatures. However, variations in the acceleration process between the different types of holes produce solar wind stream velocities which greatly differ from hole to hole. *Zurbuchen et al.* [2002] used Ulysses/SWICS data to study the evolution of the solar wind composition throughout the solar cycle. They showed that the apparent bimodal nature of the solar wind during solar minimum does not persist during solar maximum, at least with respect to solar wind speed and charge-state distributions. They reported a higher charge-state ratio in coronal-hole-associated wind during solar maximum and concluded that this is consistent with theories in which the solar wind originates from closed magnetic loops that reconnect with open field lines [*Fisk et al.*, 1999].

[6] In a series of papers, data from the Ultraviolet Coronograph Spectrometer (UVCS) on SOHO were used to derive plasma parameters of the solar minimum north polar coronal hole, a solar maximum equatorial hole and a solar maximum high-latitude coronal hole [*Kohl et al.*, 1998; *Miralles et al.*, 2001a, 2001b]. These studies indicate that ion perpendicular kinetic temperatures observed in the polar coronal hole at solar minimum are higher than in the equatorial coronal hole near solar maximum but comparable to the high-latitude coronal hole.

[7] In this paper, we investigate small-scale coronal holes observed during the maximum phase of solar cycle 23 at low to high latitudes. We use data from the Solar Wind Ion Composition Spectrometer (SWICS) and the magnetometer on Ulysses to identify coronal hole streams in interplanetary space and to relate them to coronal holes seen in Kitt Peak synoptic maps. For the identified coronal holes and their associated solar wind streams we derive interplanetary and solar surface/corona properties and compare them with characteristic parameters of the large polar coronal holes observed during solar minimum. Specifically, we concentrate on the O^{7+}/O^{6+} charge-state ratio as a proxy for the coronal temperature and on the solar wind speed representing the kinetic properties of the coronal hole streams. We complement the interplanetary observations with estimates of the coronal hole area, coronal hole magnetic flux, and flux density derived from Kitt Peak magnetic synoptic charts.

2. Data Description

[8] The Solar Wind Ion Composition Spectrometer (SWICS) on board Ulysses combines an electrostatic deflection system with a time of flight unit and a solid state detector to measure the mass, charge, and energy of thermal solar wind ions. The instrument is well suited to determine the solar wind elemental composition and the charge-state distributions of heavy solar wind ions as well as proton and alpha particle speed, density, and temperature. The SWICS instrument is described in detail by *Gloeckler et al.* [1992]. For the present study the solar wind proton speed and the oxygen charge-state ratio O^{7+}/O^{6+} are used. The charge-state ratio O^{7+}/O^{6+} allows the so-called freezing-in temperatures to be estimated. These are related to coronal temperatures in the source region of the solar wind. Specifically, charge-state ratios are a good indicator of coronal temperatures in the fast coronal hole streams [*Geiss et al.*, 1995; *von Steiger et al.*, 2000]. A detailed description of the method used to derive the O^{7+}/O^{6+} ratio including instrumental errors is given by *von Steiger et al.* [2000].

[9] The Ulysses observations are complemented by information on the coronal hole area, coronal hole magnetic flux and average flux density (i.e., spatially averaged field strength) derived from observations made at Kitt Peak. Synoptic charts of coronal holes are inferred from He I 1083 nm data, and magnetic field synoptic charts from daily magnetograms. Each synoptic chart represents one Carrington rotation of the Sun. The original observations were made with 1 arc sec pixels and then converted to daily, low resolution, maps in a Carrington longitude versus sine latitude format. The following corrections are applied to the magnetic field synoptic Charts: (1) On the generally-made assumption that the fields are perpendicular to the solar surface, the observed field strengths are divided by

cosine of latitude; (2) The magnetograph signal very close to the poles can be very noisy or even missing. In these cases the measured signal is replaced by a cubic spline fit to valid values in the polar regions. Coronal hole boundaries are identified on the He I 1083 nm synoptic maps, from which the coronal hole areas are estimated. Within the coronal hole boundaries the total magnetic flux and average flux density are derived from the magnetic synoptic charts.

[10] The present study is based on observations made between 1992 and 2002. A general overview is provided by Figure 1. Figure 1a shows the heliographic latitude range scanned by Ulysses and the variation of sunspot number over the solar cycle during this time. In the declining phase of the last solar cycle Ulysses was in the southern hemisphere, ascending in latitude toward the south polar region of the heliosphere. Ulysses reached its highest southern latitude of 80° in 1994. The fast latitude scan in 1994/1995 at perihelion took Ulysses from the south into the north polar regions of the heliosphere in just a few months. During the minimum phase of the solar cycle the spacecraft descended again from high northern latitudes toward the ecliptic. Ulysses completed its first orbit with the crossing of the ecliptic plane in 1998, and began the second slow latitude scan of the southern heliosphere, this time during solar activity maximum. At the end of 2000 Ulysses again reached southern latitudes of 80°. Following the second fast latitude scan, northern latitudes of 80° were reached at the end of 2001.

[11] Figure 1b shows 10-day averages of the O^{7+}/O^{6+} charge-state ratio and the solar wind speed measured by SWICS during this time interval. At high latitudes Ulysses observed the uniform solar wind emanating from the large polar coronal holes which existed throughout the declining/minimum phase of solar cycle 22. This polar coronal hole wind is much faster (~760 km/s) than the solar wind at low latitudes [*Woch et al.*, 1997; *McComas et al.*, 2000] and the O^{7+}/O^{6+} ratio is considerably reduced compared to the streamer belt wind, pointing to low coronal temperatures in its source region [*von Steiger et al.*, 1997; *Zhang et al.*, 2002]. During the second southern latitude scan from 1998 onward Ulysses did not encounter any persistent high-speed/low-temperature streams. This is consistent with the Kitt Peak observations which showed that in the rising/maximum phase of solar cycle 23 the large polar coronal holes had disappeared. Instead, small-scale coronal holes were observed at all latitudes [*Wang et al.*, 2000b] which formed and dissolved again on time scales of one to a few solar rotations.

[12] In the following sections we identify solar wind streams in interplanetary space emanating from these small-scale coronal holes using SWICS observations made between mid-1998 and mid-2001. We derive their interplanetary and solar surface/coronal properties and compare them with those of the large polar coronal holes observed during solar minimum.

3. Identification of Coronal Hole Streams

[13] The solar wind emanating from the large polar coronal holes is uniquely characterized by a high solar wind velocity and a low freezing-in temperature. We thus assume that the most appropriate and unambiguous way to identify

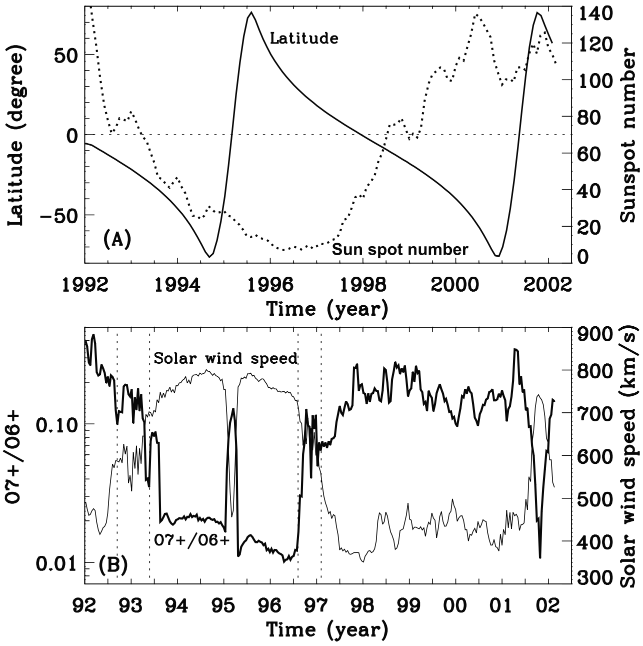

Figure 1. Ulysses heliographic latitude and sunspot number (top) and solar wind speed (light curve) and O^{7+}/O^{6+} charge-state ratio (heavy) measured by SWICS/Ulysses (bottom) from 1992 to 2002.

the solar wind streams emanating from the small coronal holes during solar maximum is to search for time intervals with enhanced solar wind speed and a correspondingly reduced freezing-in temperature compared to the ambient solar wind [see also, *McComas et al.*, 2002]. We visually inspected time series of 15-hour-averages of the solar wind speed and the O^{7+}/O^{6+} charge-state ratio and identified 37 events as possible candidates for coronal hole streams. In all these stream intervals the solar wind speed is significantly above and the O^{7+}/O^{6+} ratio significantly below values observed before and after the stream intervals. The rise in solar wind speed and corresponding drop in the O^{7+}/O^{6+} charge-state ratio occurs on short time scales within a few measurement cycles of the instrument, thus yielding sharp boundaries at the interfaces between the potential coronal hole streams and the ambient solar wind. Figure 2 shows the variation of the charge-state ratio and the solar wind velocity in the 3-year interval from mid-1998 to mid-2001 with the 37 selected intervals. The use of 15-hour averaged values was required to sufficiently reduce statistical uncertainties in the O^{7+}/O^{6+} ratio. At the same time, however, this choice introduces a bias regarding the size of the identified coronal holes. Streams from the smallest holes will escape identification. By invoking not only a solar wind speed increase but also a simultaneous drop in the charge-state ratio as identification criterion we exclude solar wind disturbances produced by other sources, like coronal mass ejections (CMEs), which do not show the characteristic anticorrelation between the two parameters.

[14] In order to verify whether the 37 events are related to coronal holes we estimated their source location on the Sun by using a simple ballistic, constant-velocity approach to map their interplanetary observation point back to the solar surface. In addition, the predominant direction of the radial

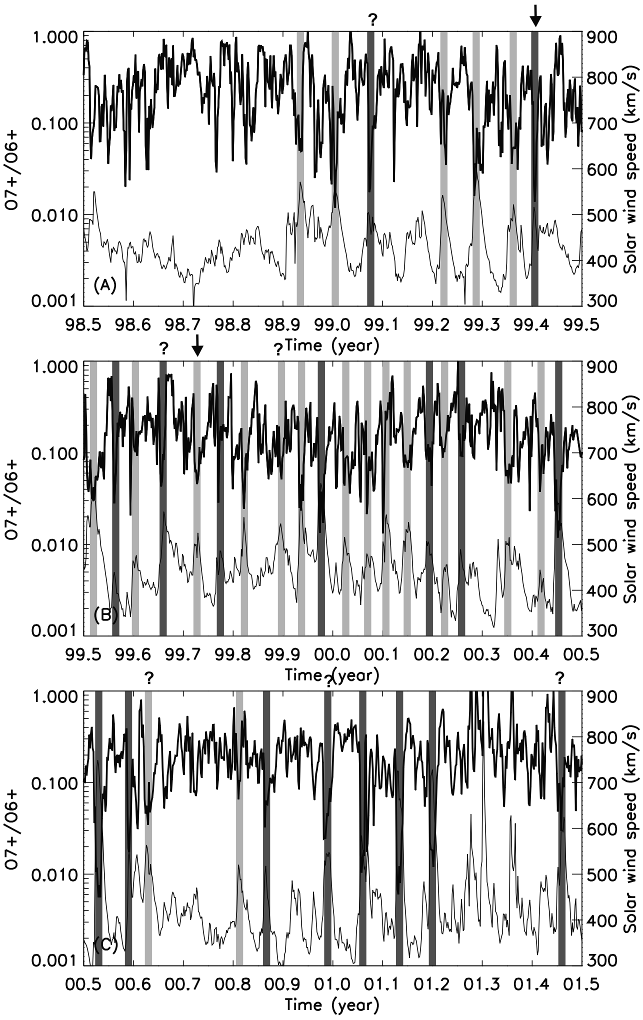

Figure 2. The solar wind speed (light curve) and O^{7+}/O^{6+} charge-state ratio (heavy) measured by SWICS/Ulysses from mid-1998 to mid-2001. 15-hour averages are displayed. Shaded areas mark solar wind streams emanating from solar maximum coronal holes. Light (heavy) shading denotes negative (positive) magnetic polarity. Question marks indicate streams with ambiguous polarity identification at Ulysses. Streams chosen as representative examples (cf. Figures 3 and 4) are marked by arrows.

component of the interplanetary magnetic field as measured by the Ulysses magnetometer [*Balogh et al.*, 1992] within the stream events was used to derive the magnetic polarity (toward or away from the Sun) of each event. It was possible to unambiguously designate a magnetic polarity to 31 out of the 37 events. Within the remaining 6 potential coronal hole streams the field direction was highly variable, making it difficult to assign a polarity to them. We then checked the Kitt Peak coronal hole and magnetic field synoptic charts for the Carrington rotation corresponding to the Ulysses observation time for any appearance of a coronal hole with the correct polarity in the vicinity of the mapped position.

[15] For all of the events with clearly defined polarity a coronal hole of correct polarity was located less than 30° Carrington longitude away from the mapped position and within an appropriate latitude range. Bearing in mind the uncertainty inherent in the mapping back procedure for events observed up to about 5 AU away from the Sun, we regard a 30° deviation as acceptable. For the majority of the stream events the mapped position even exactly coincides with a coronal hole of correct polarity. Also for the 6 events of undefined polarity a coronal hole was closely collocated with the mapped position. They are included in the study and assigned the magnetic polarity of the respective coronal holes in the synoptic maps. Thus we can conclude that each of the events could be uniquely associated with a coronal hole on the Sun.

[16] Figures 3 and 4 provide example of this result based on two arbitrarily chosen events. They are marked by arrows in Figure 2. The first coronal hole stream was observed by Ulysses on day 148 of 1999. At that time the spacecraft was at 27° southern heliographic latitude at a distance of 4.9 AU from the Sun. Figure 3 shows the solar wind speed and the O^{7+}/O^{6+} charge-state ratio derived from SWICS observations (top) together with the synoptic coro-

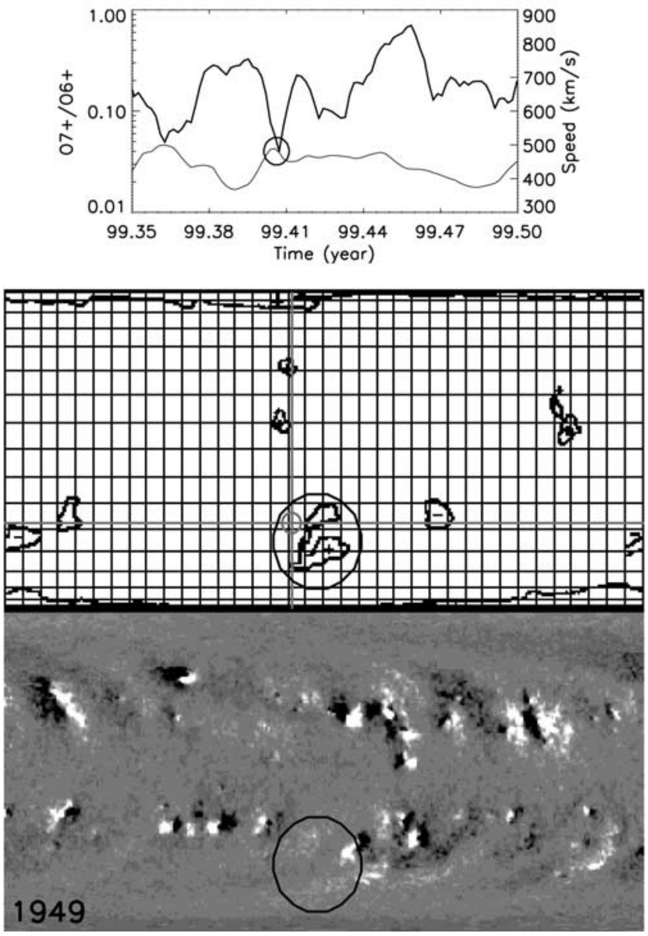

Figure 3. A coronal hole stream observed by Ulysses on day 148 of 1999. Top: Solar wind speed (light curve) and O^{7+}/O^{6+} charge-state ratio (heavy). Bottom: The synoptic coronal hole map and mean photospheric field synoptic charts of the corresponding Carrington rotation 1949. The projected position of Ulysses at the time of the coronal hole stream encounter is marked by the horizontal and vertical lines and small circle. A nearby coronal hole of correct magnetic polarity is encircled.

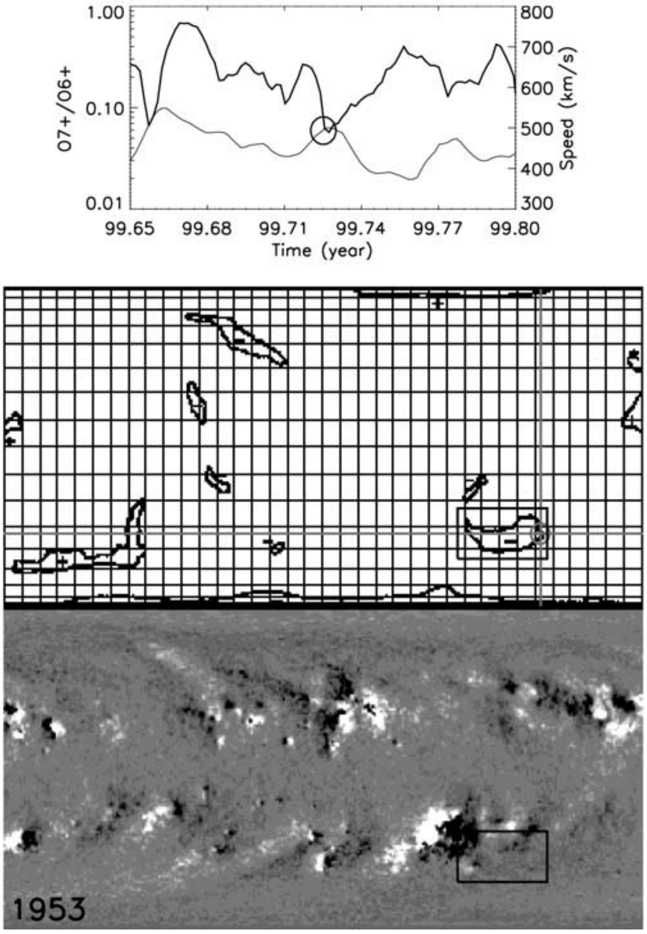

Figure 4. Same as in Figure 3, but for a stream encountered on day 265 of 1999 (corresponding to Carrington rotation 1953).

nal hole map (middle) and the corresponding photospheric field synoptic chart (bottom) for Carrington rotation 1949. From left to right, the Carrington longitude runs from 0° to 360°, while the latitude from +90° to −90° runs from top to bottom. The contours represent the boundaries of the coronal holes. The core of the coronal hole stream as seen by SWICS is marked with a circle. A solar wind speed increase from 360 km/s to nearly 500 km/s coincides with a decrease of the charge-state ratio from 0.3 to 0.04. The magnetic field is directed away from the Sun which corresponds to a positive polarity (not shown). Mapping back indicates that the fast solar wind stream emanated from the solar surface at a position of 27° southern latitude, 162° Carrington longitude, marked by the grey horizontal and vertical lines on the synoptic coronal hole map. The small circle marks the deduced source region of the solar wind stream. It is located close to a coronal hole of positive polarity (marked by a larger circle on the coronal hole map). This coronal hole can therefore be regarded as the source region of the fast solar wind stream. From the corresponding photospheric field synoptic charts, we find that the coronal hole is located near the boundary of an active region. In the same format as Figure 3, Figure 4 presents another coronal hole stream observed by Ulysses on day 265 of 1999 at a southern latitude of 34.5° and a distance of 4.5 AU. A well-defined peak in the solar wind speed of approximately 100 km/s above ambient values coincides with a sharply reduced O^{7+}/O^{6+} ratio. The magnetic field is directed toward the Sun (negative polarity). The source location is estimated at a Carrington longitude of 303° at 33° South. This location coincides with a coronal hole of negative polarity. As in the previous example the coronal hole is located close to an active region.

4. Coronal Hole Properties

[17] With SWICS/Ulysses we are able to both remotely sense coronal properties of the coronal holes and simultaneously derive in-situ kinetic properties of the solar wind emanating from the coronal holes. Figure 5 compares the small-scale coronal holes observed with Ulysses during solar maximum with the minimum phase large polar coronal holes. It shows the O^{7+}/O^{6+} charge-state ratio, which serves as a proxy for the coronal hole temperature, versus the solar wind speed representative of the solar wind properties. Furthermore, the coronal holes are distinguished on the figure with respect to their magnetic polarity. For periods in which Ulysses was permanently immersed in the southern or northern polar coronal hole streams (08.1993 to 01.1995 for south; 03.1995 to 08.1996 for north) values are averaged over individual Carrington rotations. For mid-latitude observations (08.1992 to 05.1993 and 07.1996 to 01.1997), when Ulysses encountered the polar streams once per solar rotation for a limited time, one 15-hour-average per rotation comprising the core part of the polar coronal hole encounter is displayed. Similarly, for each encounter of a solar maximum hole a 15-hour-average around the core of

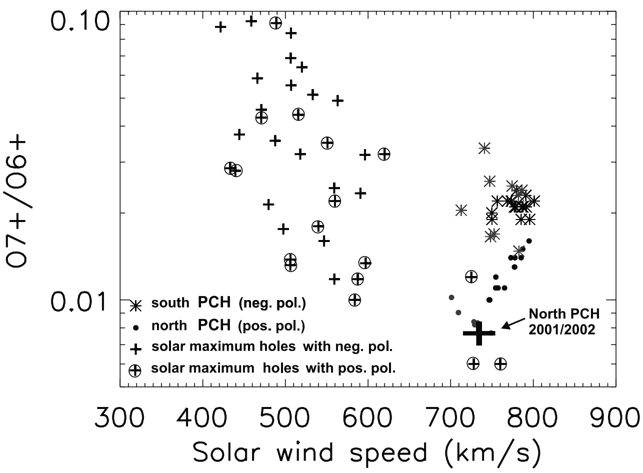

Figure 5. Scatter plot of the O^{7+}/O^{6+} charge-state ratio versus the solar wind speed measured by Ulysses in the solar wind streams emanating from coronal holes. The solar maximum holes (plus signs, negative polarity, encircled plus signs, positive polarity) are compared with the solar minimum north and south polar coronal hole (dots and stars; heavy symbols denote observations with Ulysses permanently immersed in the polar coronal hole streams, light ones short encounters of polar coronal hole streams). Also included is the coronal hole persistently observed by Ulysses at the end of 2001/beginning of 2002 above latitudes of about 70° North (heavy cross).

the stream (solar wind speed maximum, charge-state ratio minimum) is shown.

[18] In addition we have included in Figure 5 the values for a coronal hole persistently observed by Ulysses at the end of 2001/beginning of 2002 above latitudes of about 70° North. According to the Carrington maps, this coronal hole emerged at the beginning of 2001 and then evolved into a comparatively large polar coronal hole with the polarity expected for the new cycle. This hole, in its early stage, is the high-latitude solar maximum hole observed by UVCS/SOHO and discussed in the paper by *Miralles et al.* [2001b].

[19] The solar wind streams from the solar maximum coronal holes differ from the polar coronal hole streams with respect to their velocity. The speed of the solar wind from the northern and southern polar coronal hole is between 700 and 800 km/s. The speed of the solar wind streams from the solar maximum holes typically ranges from 400 to 600 km/s. Only for three coronal hole stream encounters is the speed above 700 km/s, i.e., comparable to the polar coronal hole speed. Two of these are consecutive encounters of the same hole. Likewise the speed of the solar wind stream emanating from the newly emerging north polar coronal hole is above 700 km/s.

[20] With respect to the charge-state ratios the difference is less pronounced. For the north polar coronal hole the O^{7+}/O^{6+} ratio is scattered around a value of 0.01, while for the south polar coronal hole around 0.02 (see *Zhang et al.* [2002] for a discussion of the differences between the north and south polar holes). In the case of the solar maximum holes the O^{7+}/O^{6+} ratio ranges from even below the north polar hole values to an order of magnitude higher. However, the majority of solar maximum holes have a O^{7+}/O^{6+} ratio which is within the range covered by the O^{7+}/O^{6+} ratio of the north and south polar coronal holes. Despite the large scatter a trend toward an anticorrelation between the solar wind speed and the O^{7+}/O^{6+} ratio is discernible. This suggests an influence of coronal hole temperature on solar wind speed in the sense that a lower coronal temperature leads to a faster solar wind. However, given the scatter, this result is in need of confirmation either from other data or through an improved analysis.

[21] Of the 37 solar maximum coronal holes identified in the southern hemisphere, 17 showed a positive magnetic polarity. Nine of these were observed after May 2000, i.e, in the last third of the time interval studied. The remaining 20 events had negative polarity, but only two of these were observed after May 2000. During solar cycle 22 the polar hole in the southern hemisphere had a negative polarity. Thus a positive polarity corresponds to the polarity of the new solar cycle. The observations imply that by mid-2000 the solar magnetic field has reversed its polarity. Except for one case, solar maximum coronal holes of positive polarity (i.e. new cycle polarity) have comparatively low O^{7+}/O^{6+} ratios, which are either only slightly above or in the same range as the values found in the polar coronal hole. The two streams showing a very low ratio are also of positive polarity. For ratios considerably above the polar coronal hole values negative, old cycle, polarity holes dominate.

[22] Figure 6 summarizes the properties derived from the coronal hole and magnetic field synoptic charts. It shows scatter diagrams of coronal hole area versus magnetic flux and flux density, as well as flux versus flux density. The figure includes the polar coronal holes of cycle 22 and the small-scale solar maximum holes observed in the southern hemisphere between mid-1998 and mid-2000. It includes both solar maximum holes, whose solar wind streams were observed with Ulysses (marked by crosses), and those without an observed interplanetary signature (marked by open or filled circles).

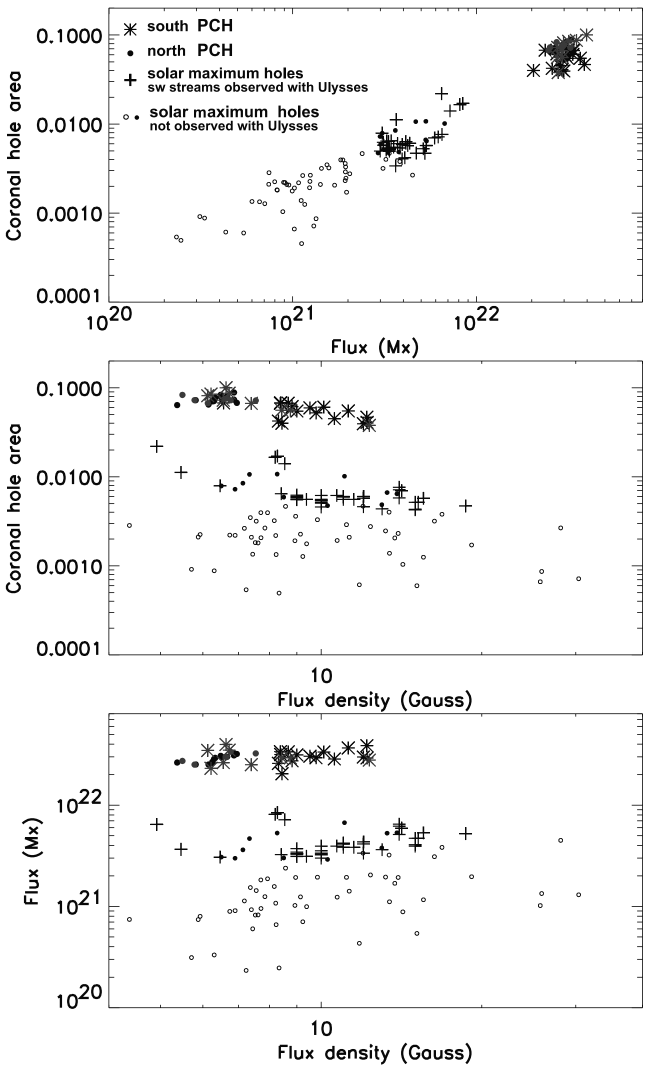

Figure 6. Scatter plots of the coronal hole area versus total emerging magnetic flux (top) and versus magnetic flux density (middle), as well as a scatter plot of total flux versus flux density (bottom). The values are derived from Kitt Peak synoptic charts. The figure includes the solar maximum holes of which solar wind streams were identified in Ulysses data (plus signs), solar maximum holes not detected with Ulysses (open and filled small circles, see text for details), and the south (stars) and north (large dots) polar coronal holes.

[23] The solar minimum polar coronal holes encompass an area one to two orders of magnitude larger than the solar maximum holes. Not surprisingly, the total magnetic flux emerging from the coronal holes increases with coronal hole size. In the scatter diagram the polar holes are consequently

clearly separated from the solar maximum holes both in size and total flux. Both quantities vary by nearly three orders of magnitude. In contrast, the average magnetic flux density varies over less than an order of magnitude. It ranges from about 4 to 30 Gauss, with the polar coronal holes scattered toward the lower and the solar maximum holes toward the higher limit of this range. This corroborates the findings by *Harvey et al.* [1982] and the recent study by *Wang et al.* [2000a]. Apart from the minor difference between the flux density of the large polar coronal holes and that of the small-scale solar maximum holes there is no obvious relation between the size of the solar maximum holes and their flux density.

[24] Figure 6 confirms that our study is biased toward relatively large coronal holes. Only streams from large-sized coronal holes were identified with Ulysses. It also shows that only a rather small number of large-sized holes were not identified with Ulysses (small filled dots). Moreover, Ulysses may not have detected these large holes, which were observed from Earth, because they were located at significantly different latitudes or longitudes from the spacecraft. Thus, they might already have disappeared during the time it took to rotate to the longitude conjugate to Ulysses. There is no apparent bias in the flux density of the coronal holes selected for analysis.

[25] Finally, Figure 7 relates the properties of the coronal holes derived from interplanetary observations to those derived from the synoptic maps. It shows scatter diagrams of the O^{7+}/O^{6+} ratio (left panel) and the solar wind speed (right panel) plotted against coronal hole area, magnetic flux density and total magnetic flux (from top to bottom). It does not reveal an unambiguous relationship between any of the quantities. The clearest sign of a possible dependence, however, (although still with some scatter) is that of wind speed on coronal hole area (and thus also on total flux). There is some indication that faster solar wind emanates from larger coronal holes. Furthermore, there is a hint of a relation between the O^{7+}/O^{6+} ratio and flux density as well as between solar wind speed and flux density. With decreasing flux density the solar wind speed appears to increase and the O^{7+}/O^{6+} ratio to drop. However, the number of cases available in this study is too small to arrive at a definite conclusion.

5. Summary and Discussion

[26] Based on SWICS/Ulysses data and Kitt Peak synoptic charts we have studied coronal holes observed during solar maximum. We focused on properties imprinted in the solar wind streams emanating from the coronal holes as well as on the properties of the coronal holes themselves. We were able to identify 37 coronal hole streams within a wide range of southern latitudes in the SWICS/Ulysses data set and to associate them with coronal holes in Kitt Peak synoptic maps. A sharp decrease of the O^{7+}/O^{6+} charge-state ratio and a simultaneous increase in solar wind speed proves to be a reliable identification criterion. The large number of identified events is sufficient to arrive at some general conclusions regarding coronal hole properties. Furthermore, in combination with previous studies on polar coronal holes during solar minimum we are now able to compare properties of coronal holes throughout the solar cycle.

[27] The polar coronal holes during solar minimum, though prominent in their stability and size, do not differ significantly from solar maximum holes in their fundamental properties. The magnetic flux density of the coronal holes derived from Kitt Peak synoptic charts varies over a relatively narrow range, from about 4 to 30 Gauss. The solar maximum coronal holes are scattered toward higher values and the solar minimum polar holes toward lower values. However, there is a considerable overlap.

[28] The oxygen charge-state ratio, a robust diagnostic of coronal conditions in the source region of the solar wind streams, is remarkably similar in the solar minimum polar holes and the solar maximum holes. This is especially true when comparing solar minimum polar holes with solar maximum holes observed at high latitudes. This latter finding confirms the result of the *McComas et al.* [2002] study on solar maximum high-latitude holes and the result of *Miralles et al.* [2001b] on the high-latitude solar maximum hole observed with UVCS/SOHO. Thus we can state that high-latitude coronal holes forming at solar maximum and the solar minimum polar coronal holes are not of a fundamentally different type. Furthermore, bearing in mind that the polar holes and specifically their freezing-in temperatures are remarkably stable over several years around solar minimum [*von Steiger et al.*, 2000; *Zhang et al.*, 2002], we can conclude that the freezing-in temperature in coronal holes observed at high solar latitudes, i.e., at latitudes above the active regions of the Sun, does not exhibit a solar cycle dependence, although the coronal hole size strongly varies between solar maximum and minimum.

[29] For the coronal holes emerging during solar maximum in the active belts of the Sun the situation is less clear. The freezing-in temperature varies considerably between individual holes. Although the majority of coronal holes still have temperatures within the range of the polar hole values, a relatively large number of coronal holes show temperatures well above polar hole temperatures. However, nearly all of the latter holes have a negative magnetic polarity. Since they are observed in the southern hemisphere this polarity corresponds to the magnetic polarity of the old cycle. Moreover, with the exception of one coronal hole observed still in the early phase of solar cycle 23, the temperatures in all other coronal hole streams having the magnetic polarity of the new cycle do not significantly exceed the temperature range of the polar coronal holes. Thus coronal holes emerging shortly before the transition of the solar magnetic field to the new polarity seem to have higher freezing-in temperatures.

[30] In contrast to the conditions in the corona, the kinetic properties of the solar wind emerging from the solar minimum polar holes and solar maximum coronal holes differ significantly. With the exception of the solar wind streams emanating from 2 southern high-latitude coronal holes and the stream from the north polar coronal hole emerging in 2001, all other coronal hole streams have velocities well below those of the solar minimum polar coronal hole streams. Their velocities are typically between 400 and 600 km/s compared to the 750 km/s of the polar holes. This leads to a pronounced gap in the velocity distribution of coronal hole streams extending from about 620 to 720 km/s. We suggest that these greatly different velocities do not reflect a fundamental difference in the coronal conditions but

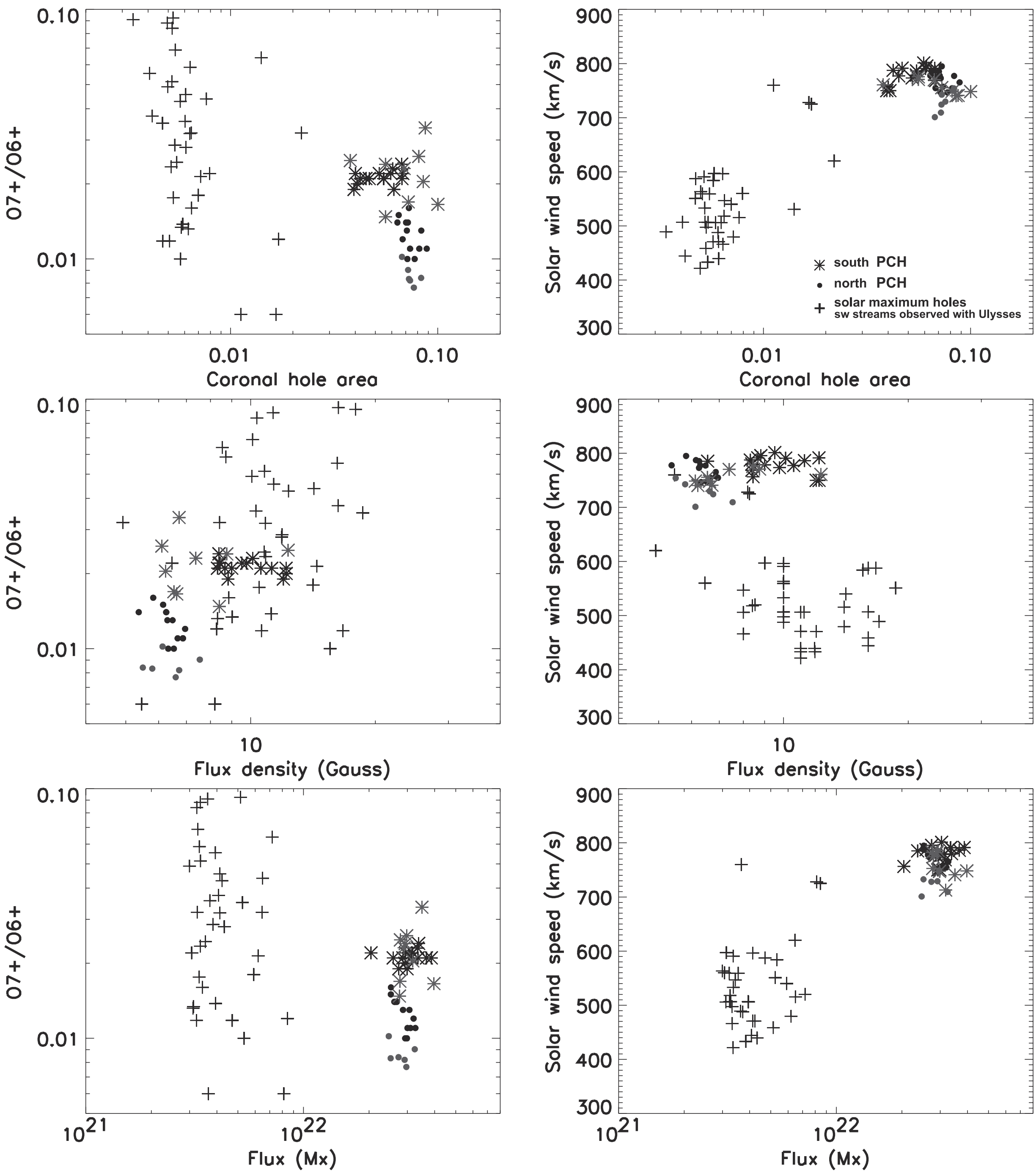

Figure 7. Coronal hole parameters derived from SWICS/Ulysses compared to those derived from Kitt Peak synoptic charts (symbols as in Figure 6). Left: The O^{7+}/O^{6+} charge-state ratio versus coronal hole area, flux density, and total flux (from top to bottom). Right: the same but for the solar wind speed.

rather that they are due to variation in the acceleration process [see also *McComas et al.*, 2002] or due to deceleration through interaction with slow solar wind during propagation to the spacecraft. The tendency for the small coronal holes at sunspot maximum to produce slower wind than the large polar holes near minimum is in good agreement with predictions by the wind speed-expansion factor relationship. Small holes are characterized by rapidly diverging field lines and generate slower wind, whereas inside the large polar holes field lines are slowly diverging and produce faster wind [*Wang et al.*, 1997]. Taking into account the effects of interactions between fast and slow wind, speeds of about 600 km/s were deduced for the small solar maximum holes compared to 750 km/s for solar minimum polar holes [*Wang and Sheeley*, 1997]. Furthermore, we found that all the streams with velocities below 620 km/s emanate from coronal holes emerging within the active belt of the Sun (cf. Figures 4 and 5). These holes are either directly adjacent (31 holes) or in close vicinity (3 holes) to one or more active regions. The solar wind streams with velocities above 720 km/s are all emanating from coronal holes located at high latitudes far away from any active region. Again this is in qualitative agreement with the finding of *Wang and Sheeley* [1997], that wind streams at maximum are considerably faster in the absence of interactions.

[31] **Acknowledgments.** NSO/Kitt Peak data used here are produced cooperatively by NSF/NOAO, NASA/GSFC, and NOAA/SEL. The maps of coronal holes were prepared by Drs. Karen Harvey and Frank Recely as part of an NSF grant. JZ was supported by the Ministry of Science and Technology of China under Grant G2000078404. This work was partly supported by the Deutsches Zentrum für Luft- und Raumfahrt e.V.(DLR).

[32] Shadia Rifai Habbal thanks Yi-Ming Wang and another referee for their assistance in evaluating this paper.

References

Balogh, A., et al., The magnetic field investigation on the Ulysses mission: Instrumentation and preliminary scientific results, *Astron. Astrophys. Suppl. Ser.*, *92*, 221, 1992.

Fisk, L. A., T. H. Zurbuchen, and N. A. Schwadron, The acceleration of the fast solar wind by the emergence of new magnetic flux, *J. Geophys. Res.*, *104*, 19,765, 1999.

Forsyth, R. J., A. Balogh, T. S. Horbury, G. Erdös, E. J. Smith, and M. E. Burton, The heliospheric magnetic field at solar minimum: Ulysses observations from pole to pole, *Astron. Astrophys.*, *316*, 287, 1996.

Geiss, J., et al., The Southern high-speed stream: Results from the SWICS Instrument on ULYSSES, *Science*, *268*, 1033, 1995.

Gloeckler, G., et al., The Solar Wind Ion Composition Spectrometer, *Astron. Astrophys. Suppl. Ser.*, *92*, 267, 1992.

Harvey, K. L., N. R. Sheeley Jr., and J. W. Harvey, Magnetic measurements of coronal holes during 1975–1980, *Sol. Phys.*, *79*, 149, 1982.

Kohl, J. L., et al., UVCS/SOHO empirical determination of anisotropic velocity distributions in the solar corona, *Astrophys. J.*, *501*, L127, 1998.

Krieger, A. S., A. F. Timothy, and E. C. Roelof, A coronal hole and its identification as the source of a high velocity solar wind stream, *Sol. Phys.*, *29*, 505, 1973.

Luhman, J. G., Y. Li, C. N. Arge, P. R. Gazis, and R. Ulrich, Solar cycle changes in coronal holes and space weather cycles, *J. Geophys. Res.*, *107*(A8), 1154, doi:10.1029/2001JA007550, 2002.

McComas, D. J., et al., Solar wind observations over Ulysses' first full polar orbit, *J. Geophys. Res.*, *105*, 10,419, 2000.

McComas, D. J., H. A. Elliott, and R. von Steiger, Solar wind from high-latitude coronal holes at solar maximum, *Geophys. Res. Lett.*, *29*(9), 1314, doi:10.1029/2001GL013940, 2002.

Miralles, M. P., S. R. Cranmer, A. V. Panasyuk, M. Romoll, and J. L. Kohl, Comparison of empirical models for polar and equatorial coronal holes, *Astrophys. J.*, *549*, L257, 2001a.

Miralles, M. P., S. R. Cranmer, and J. L. Kohl, Ultraviolet coronagraph spectrometer observations of a high-latitude coronal hole with high oxygen temperatures and the next solar cycle polarity, *Astrophys. J.*, *560*, L193, 2001b.

von Steiger, R., J. Geiss, and G. Gloeckler, Composition of the solar wind, in *Cosmic Winds and the Heliosphere*, edited by J. R. Jokipii, C. P. Sonet, and M. S. Giampapa, pp. 581–616, Univ. of Ariz. Press, Tucson, 1997.

von Steiger, R., N. A. Schwadron, L. A. Fisk, J. Geiss, G. Gloeckler, S. Hefti, B. Wilken, R. F. Wimmer-Schweingruber, and T. H. Zurbuchen, Composition of quasi-stationary solar wind flows from Ulysses/Solar Wind Ion Composition Spectrometer, *J. Geophys. Res.*, *105*, 27,217, 2000.

Wang, Y.-M., and N. R. Sheeley Jr., The high-latitude solar wind near sunspot maximum, *Geophys. Res. Lett.*, *24*, 3141, 1997.

Wang, Y.-M., N. R. Sheeley Jr., J. L. Phillips, and B. E. Goldstein, Solar wind stream interactions and the wind speed-expansion factor relationship, *Astrophys. J.*, *488*, L51, 1997.

Wang, Y.-M., J. Lean, and N. R. Sheeley Jr., The long-term variability of the Sun's open magnetic flux, *Geophys. Res. Lett.*, *27*, 505, 2000a.

Wang, Y. M., et al., Evolution of coronal stream structure during the rising phase of solar cycle 23, *Geophys. Res. Lett.*, *27*, 149, 2000b.

Woch, J., et al., SWICS/Ulysses observations: The three-dimensional structure of the heliosphere in the declining/minimum phase of the solar cycle, *Geophys. Res. Lett.*, *24*, 2885, 1997.

Zhang, J., J. Woch, S. K. Solanki, and R. von Steiger, The Sun at solar minimum: North-south asymmetry of the polar coronal holes, *Geophys. Res. Lett.*, *29*(8), 1236, doi:10.1029/2001GL014471, 2002.

Zurbuchen, T. H., L. A. Fisk, G. Gloeckler, and R. von Steiger, The solar wind composition throughout the solar cycle: A continuum of dynamic states, *Geophys. Res. Lett.*, *29*(9), 1352, doi:10.1029/2001GL013946, 2002.

S. K. Solanki, J. Woch, and J. Zhang, Max-Planck-Institut für Aeronomie, Katlenburg-Lindau, D-37191, Germany. (solanki@linmpi.mpg.de; woch@linmpi.mpg.de; zhangj@linmpi.mpg.de)

R. von Steiger, International Space Science Institute, Hallerstr. 6, 3012 Bern, Switzerland.

R. Forsyth, The Blackett Laboratory, Imperial College, London SW7 2BW, U.K.